Contrib Mineral Petrol (1998) 130: 176–186

Pauline Thompson · Ian Parsons · Colin M. Graham
Brian Jackson

The breakdown of potassium feldspar at high water pressures

Received: 6 May 1997 / Accepted: 2 October 1997

Abstract The equilibrium position of the reaction between sanidine and water to form "sanidine hydrate" has been determined by reversal experiments on well characterised synthetic starting materials in a piston cylinder apparatus. The reaction was found to lie between four reversed brackets of 2.35 and 2.50 GPa at 450 °C, 2.40 and 2.59 GPa at 550 °C, 2.67 and 2.74 GPa at 650 °C, and 2.70 and 2.72 GPa at 680 °C. Infrared spectroscopy showed that the dominant water species in sanidine hydrate was structural H_2O. The minimum quantity of this structural H_2O, measured by thermogravimetric analysis, varied between 4.42 and 5.85 wt% over the pressure range of 2.7 to 3.2 GPa and the temperature range of 450 to 680 °C. Systematic variation in water content with pressure and temperature was not clearly established. The maximum value was below 6.07 wt%, the equivalent of 1 molecule of H_2O per formula unit. The water could be removed entirely by heating at atmospheric pressure to produce a metastable, anhydrous, hexagonal $KAlSi_3O_8$ phase ("hexasanidine") implying that the structural H_2O content of sanidine hydrate can vary. The unit cell parameters for sanidine hydrate, measured by powder X-ray diffraction, were $a = 0.53366$ (± 0.00022) nm and $c = 0.77141$ (± 0.00052) nm, and those for hexasanidine were $a = 0.52893$ (± 0.00016) nm and $c = 0.78185$ (± 0.00036) nm. The behaviour and properties of sanidine hydrate appear to be analogous to those of the hydrate phase cymrite in the equivalent barium system. The occurrence of sanidine hydrate in the Earth would be limited to high pressure but very low temperature conditions and hence it could be a potential reservoir for water in cold subduction zones. However, sanidine hydrate would probably be constrained to granitic rock compositions at these pressures and temperatures.

P. Thompson (✉)[1] · I. Parsons · C.M. Graham
Department of Geology and Geophysics, University of Edinburgh, West Mains Road, Edinburgh, EH9 3JW, Scotland

B. Jackson
The Royal Museum of Scotland, Chambers Street, Edinburgh, EH1 1JF, Scotland

Present address:
[1] Department of Physics and Astronomy, University of Glasgow, Glasgow, G12 8QQ, Scotland,
Fax: ++44-141-330-4464, e-mail: P. Thompson@physics.gla.uk

Editorial responsibility: J. Hoefs

Introduction

Potassium feldspar is an abundant mineral in the Earth's crust and breaks down to form a wadeite type phase between 3 GPa at 700 °C and 6 GPa at 1400 °C under anhydrous conditions (Kinomura et al. 1975). At high partial pressures of water, potassium feldspar reacts to form a hydrated phase ($KAlSi_3O_8 \cdot nH_2O$; Seki and Kennedy 1964a), here referred to as sanidine hydrate although previously it has also been referred to as K-cymrite (Massonne 1992). Seki and Kennedy determined the pressure and temperature required to synthesise the hydrated phase but did not attempt to determine the equilibrium position of the reaction. The similarity of the ionic radii of barium and potassium ions suggests that sanidine hydrate may behave in a similar manner to the barium feldspar hydrate, cymrite ($BaAl_2Si_2O_8 \cdot nH_2O$) (e.g. Seki and Kennedy 1964b; Drits et al. 1975; Nitsch 1980; Moles 1985; Graham et al. 1992; Viswanathan et al. 1992; Hsu 1994). Graham et al. (1992) investigated the stability of cymrite and showed that the water content (nH_2O) varied between one molecule of H_2O per formula unit ($BaAl_2Si_2O_8 \cdot H_2O$), at higher pressures and lower temperatures, and anhydrous hexagonal hexacelsian ($BaAl_2Si_2O_8$), at low pressures and high temperatures. Viswanathan et al. (1992) confirmed that this was a solid solution by showing that the cell parameters of intermediates between cymrite and hexacelsian varied continuously between the cell parameters for each end member. By analogy, if sanidine hydrate can also contain a large proportion of structural water it may contribute to the storage of fluids in subducting slabs, the lower crust or the upper mantle.

In the present study these questions were addressed by investigating experimentally the reaction between sanidine and water to form sanidine hydrate,

$$KAlSi_3O_8 \cdot nH_2O \rightleftharpoons KAlSi_3O_8 + nH_2O$$
$$\text{sanidine hydrate} \rightleftharpoons \text{sanidine} + \text{water} \quad (1)$$

The nature of structural water within sanidine hydrate was observed with infrared spectroscopy and an attempt made to quantify the structural water at a number of pressures and temperatures by thermogravimetric analysis. The cell parameters of the sanidine hydrate and of the dehydrated product of thermogravimetric analysis (referred to as hexasanidine) were measured. The geological implications of sanidine hydrate stability at high pressure and temperature were considered. The present study is an extension of the preliminary results outlined in Thompson (1994) including a subsequent refinement in the pressure calibration.

Experimental and analytical techniques

Starting materials for high pressure experiments

Starting materials were synthesised from a gel of $KAlSi_3O_8$ composition, prepared by the method of Hamilton and Henderson (1968) and kindly donated by Dr D.L. Hamilton. Sanidine was synthesised at 0.1 GPa and 750 °C in an externally heated gas pressure vessel, and sanidine hydrate at 3.0 GPa and 550 °C in a piston cylinder apparatus. Synthesis products were mixed in the proportions 40% sanidine hydrate to 60% sanidine (subsequently referred to as PTmix) for use in reversal experiments. All high pressure runs also contained between 6.07 and 9.0 wt% of doubly deionised and distilled water (6.07 wt% being the amount of water equivalent to 1 molecule of H_2O per formula unit of sanidine hydrate [$KAlSi_3O_8 \cdot H_2O$]). In all synthesis and reversal experiments there was always free water remaining at the end of the experiment and hence 6.07 wt% was thought to be a sufficient quantity to saturate the solid system. Water contents were minimised since, with a large excess of water, a significant amount of the starting material could dissolve, probably incongruently, in the vapour phase (Stern and Wyllie 1981). Low pressure experiments contained 2–3 wt% of doubly deionised and distilled water in order to increase crystallisation rate.

Platinum capsules of similar cylindrical flat-ended design and varying sizes were used in all the high pressure experiments. Synthesis of sanidine hydrate was carried out using capsules of 4 mm outside diameter and 0.1 mm wall thickness. The reversal experiments were performed in capsules of 3 mm outside diameter in order to conserve starting material. Sanidine was synthesised at lower pressures in capsules 30 to 40 mm long, with 4 mm outside diameter and 0.07 mm wall thickness.

High pressure experiments using the piston cylinder apparatus

The capsule containing the sample was held within the centre of a graphite furnace using hot-pressed boron nitride pieces as spacers (i.e. BN with B_2O_3 as a binder). A disc of crushable alumina, approximately 0.9 mm thick, was placed on top of the capsule. The thermocouple was made of platinum/rhodium wire within a 2-bore alundum thermocouple sheath. Soft-fired synthetic pyrophyllite held the thermocouple in position in the top of the furnace. A short (1 mm) length of boron nitride sleeve was used around the tip of the thermocouple to protect it in all reversal experiments. Surrounding the graphite furnace was a sleeve of NaCl that, like BN, should act as a frictionless pressure medium. At the bottom end the salt sleeve was made longer than the graphite furnace (1.5 mm), with the inset of a steel ring, to allow for the extra compressibility of the salt.

Initially the pressure was raised to the run pressure and left to stabilise for at least two hours during which the pressure dropped by up to 0.15 GPa. During the heating process the pressure usually increased to 0.05 GPa above the run pressure. Oil pressure was then bled off during the first hour or so of the experiment until the system stabilised. Subsequently pressure was adjusted slightly as the temperature in the room fluctuated or small leakages lowered the pressure. This procedure probably produced "piston-out" conditions as the salt expanded. However, the exact position of the piston remained uncertain. In some longer runs pressure fell slightly, due to leakages or a drop in ambient temperatures, possibly resulting in "piston-in" conditions. In theory this was not important provided little pressure correction was required during the run (see below) and hence the hysteresis in the pressure was negligible.

The applied pressure was measured using an oil-filled Heise gauge. The cell used in the pressure-temperature range of the experiments was calibrated against the quartz–coesite reaction to determine the true pressure on the sample. A small pressure correction was measured by calibration against the quartz–coesite reaction (Thompson 1995). The pressures quoted in the present paper were corrected to those of Bohlen and Boettcher (1982) for the quartz–coesite reaction using the equation

$$P_{true} = -2.2429 + 2.8906P_{obs} - 0.3971P_{obs}^2,$$

[where P_{true} = corrected pressure (GPa), and P_{obs} = pressure measured in apparatus (GPa)]. The more recent work of Bose and Ganguly (1995) shows the quartz–coesite reaction to be 1.5 GPa higher than found by Bohlen and Boettcher (1982). The use of the quartz–coesite reaction of Bose and Ganguly would require a pressure correction of opposite sign and the correction would be greater at lower pressures and temperatures. The error in estimation of the pressure, once the correction to Bohlen and Boettcher's work had been applied, was within ±0.05 GPa.

The temperature within the cell was measured to ±1 °C using a $Pt/Pt_{87}Rh_{13}$ thermocouple junction referenced against a "cold junction" maintained at 0 °C in an ice-water bath. It was automatically controlled to within ±2 °C by a Eurotherm controller. The additional uncertainty of the effect of pressure on the temperature reading was unknown and was presumed to be negligible.

The major factor affecting temperature measurement was the thermal gradient in the apparatus, the effects of which were minimised in three ways:

1. The capsule was placed in the central part of the furnace
2. The length of the capsule was less than 5 mm, restricting the thermal gradient to <5 °C (N. Odling, personal communication).
3. The capsule was loaded with the thinner crimp at the top so that the distance between the thermocouple bead and the sample was always at a minimum.

The temperature of the sample was within ±10 °C of the thermocouple reading.

Synthesis and structural state of sanidine starting material

Sanidine starting material was synthesised in externally heated 30 cm "Tuttle" cold seal vessels using an argon gas pressure medium at 0.1 GPa and 750 °C, in 24 hour runs. Subsequent experiments were carried out down to 450 °C at up to 4.5 GPa, in runs of up to 168 hours. Although the temperature-dependence of the equilibrium degree of Si, Al ordering is not well known, it is probable that most ordering (the low sanidine–microcline transformation) takes place in the 500–470 °C range at 0.1 GPa (see Brown and Parsons, 1989, Fig. 3 and accompanying discussion; Carpenter and Salje 1994). The pressure-dependence of the trans-

formation is not known directly but, for albite, the high–low transition moves to higher temperature with increasing pressure by about 30 °C GPa^{-1}. It is therefore possible that the stable equilibrium low sanidine–microcline phase transformation will intersect the sanidine–sanidine hydrate reaction (Fig. 1) at about 550 °C. As temperature increases, the equilibrium degree of T1/T2 order decreases more slowly, and low sanidine will be the stable feldspar over the temperature range of the experiments described below. However, in practice the slow ordering rates in K-feldspar make it probable that the feldspars in all the present experiments were relatively highly disordered. This was confirmed using X-ray diffraction and the "three-peak" method of Wright (1968), which showed that the starting material sanidines produced at 0.1 GPa were very close to high sanidine (within 0.03°2θ, CuKα). The product sanidines present after the high pressure runs were slightly ordered, extending to a point about halfway between high and low sanidine on Wright's diagram (1968, Fig. 3). Strictly speaking, the equilibrium shown on Fig. 1 is metastable, with respect to Si, Al order in the feldspar, throughout the entire range shown; at stable equilibrium it would show an inflection in the region of 550 °C. However, it is a good approximation to a metastable high sanidine–sanidine hydrate equilibrium because it is unlikely that any effect of ordering occurring during the experiments would be greater than the width of the experimental brackets. It is possible that ordering may also occur in the sanidine hydrate phase.

Examination of run products

After the experiment, the capsule was extracted, cleaned, weighed, pierced and heated to 100 °C for a few hours to test for capsule integrity. Samples were ground under acetone in an agate mortar and pipetted onto a slide for mounting in the powder X-ray diffractometer. Acetone was used as it evaporates quickly allowing less time for crystals to orientate preferentially.

Optical examination of the fine-grained run products under appropriate refractive index oil was difficult, but where larger crystals were present it was possible to distinguish between hexagonal sanidine hydrate with straight extinction and monoclinic sanidine with inclined extinction. Coesite, although not abundant, was readily distinguished by its high relief.

A Philips PW 1800 X-ray diffractometer ($CuK\alpha_1$, 40 kV, 50 mA) was used for routine product characterisation. In order to identify the direction of reaction in a reversal experiment the mixture of sanidine and sanidine hydrate was scanned using XRD both before and after the experiment. Each scan was repeated using ten different sample mounts, and average peak heights of the peaks at 27.50°2θ (sanidine) and at 33.58°2θ (sanidine hydrate) were taken. To be certain the reaction direction was correct, only changes in relative peak heights that indicated a change in the proportions of the phases of greater than 15% were used. All samples were mounted using the same method so any effects caused by preferred orientation should be consistent throughout.

Infrared spectroscopy

The instrument bench used was a Nicolet 510P Fourier Transform Infrared (FTIR) spectrophotometer. A helium/neon laser was used which measured between 5800 cm^{-1} and 200 cm^{-1} with a CsI beam splitter and a CsI detector. Each spectrum was measured using 128 scans at a resolution of 2 cm^{-1}. The sample was mounted in a potassium bromide disc and the system purged with dry CO_2-free air.

Thermogravimetric analysis

A Thermal Analyst 2000, STD 2690 Simultaneous DTA-DTG (based at the Department of Chemistry, University of St Andrews) was used for thermogravimetric analysis. The experimental programme involved holding the sample at room temperature for 10 minutes to allow the balance to stabilise before steadily heating the sample at a fixed rate of 10 °C per minute up to the maximum temperature. It was then held at this temperature for 10 minutes before fan cooling to room temperature. The initial samples were run up to a temperature of 1000 °C.

The thermogravimetric results showed variations between different aliquots of the same sample which exceeded normal experimental uncertainties. These significant variations were probably due to the nature of the samples rather than the measuring equipment. Had there been any contamination of the sanidine hydrate with other anhydrous phases the percentage weight loss would have appeared lower. Three possible sources of contamination could account for these anomalies. Firstly, coesite was a minor by-product in all of the high pressure experiments that produced sanidine hydrate (Table 2). Rough calibration of the peak height of coesite using powder XRD showed that the quantity of coesite was approximately 3 wt% or less. Samples which were not synthesised in the coesite stability field probably would have contained similar amounts of quartz that was difficult to detect in the presence of sanidine. Secondly, it is possible that the sanidine hydrate or sanidine was not entirely crystalline. This possibility was hard to test optically. All samples contained some material with a brownish hue but it was not possible to prove that it was amorphous. The third source of contamination was platinum flaked from the capsule walls when the sample was extracted after piston cylinder experiments. Atomic absorption was used to attempt to quantify the amount of platinum in some samples. Run products were found to contain amounts of platinum that would have reduced the weight loss seen in thermogravimetric analysis by 10–15%. Hence the figures obtained for weight loss are minimum values.

Techniques used in calculating cell parameters

For accurate crystallographic work the X-ray scan was set to run from 2 °2θ to 140 °2θ using a step size of 0.015°2θ and a measurement time of 3 seconds per step on a spinning sample that contained quartz as an internal standard.

The cell parameters of sanidine hydrate and hexasanidine were refined from an initial starting point of Seki and Kennedy's (1964a) values for the cell parameters of $a = 0.533$ nm and $c = 0.770$ nm using a hexagonal primitive cell. The structure may be monoclinic but in cymrite the weak satellite reflections that showed the monoclinic symmetry were only apparent in single crystal X-ray patterns (Drits et al. 1975). The cymrite cell parameters of Viswanathan et al. (1992) were all calculated using this pseudohexagonal symmetry.

The X-ray diffraction patterns used for unit cell refinements did not always contain the same set of peaks. This may be due to preferred orientation developing during the mounting procedure. In order to ensure consistency between calculations, ten prominent peaks that spanned a wide angle range and could be seen in all the spectra, were therefore chosen for cell refinement calculations. Table 1 shows the average positions of the ten peaks chosen for cell refinement of sanidine hydrate and hexasanidine. The figures for the cell parameters in Tables 5 and 6 are those generated by the program CELLREF kindly provided by Dr P. Champness.

Phase equilibrium studies

The equilibrium position of the reaction between sanidine and sanidine hydrate was determined by reversal experiments, summarised in Table 2, at a variety of pressures and temperatures on the mixture "PTmix" (Fig. 1). The equilibrium position of the reaction lies between 2.35 GPa and 2.50 GPa at 450 °C, 2.40 GPa

Table 1 Approximate positions of reflections and their indices, assigned by the Philips software, used to refine the cell parameters for the structures of sanidine hydrate and hexasanidine

Sanidine hydrate				Hexasanidine			
2θ position	*h*	*k*	*l*	2θ position	*h*	*k*	*l*
19.178	1	0	0	19.366	1	0	0
22.406	1	0	1	22.482	1	0	1
23.040	0	0	2	22.729	0	0	2
30.153	1	0	2	30.031	1	0	2
33.555	1	1	0	33.875	1	1	0
38.940	2	0	0	41.040	2	0	1
40.274	2	0	1	49.041	1	1	3
47.084	0	0	4	58.247	2	1	2
57.900	2	1	2	71.276	2	2	0
70.524	2	2	0	137.933	1	1	9

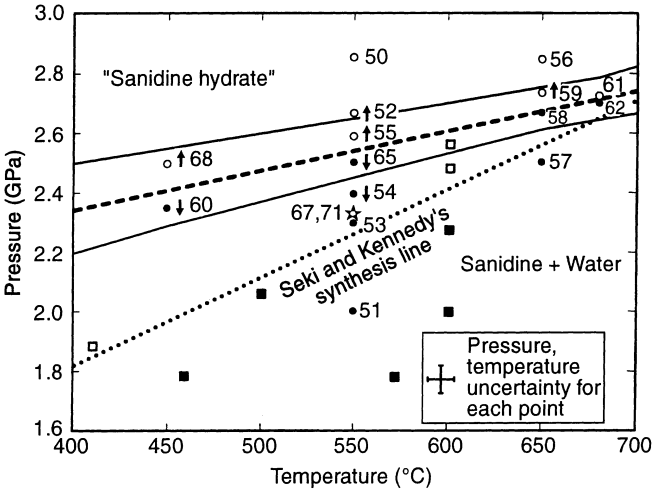

Fig. 1 Results of reversal experiments on the sanidine–"sanidine hydrate" reaction (○ = "sanidine hydrate", ● = sanidine). The *numbers* refer to the run numbers as given in Table 2. The *arrows* show the reaction direction when the reaction was not complete but was considered sufficient to determine the reaction direction. The reaction should lie in a position between the *two solid lines* e.g. in the position of the *dashed line*. The synthesis points of Seki and Kennedy (1964a) are shown for comparison (□ = sanidine hydrate, ■ = sanidine). Numbered points marked ☆ show run conditions of present experiments to investigate the metastable crystallisation behaviour of sanidine hydrate

and 2.59 GPa at 550 °C, 2.67 GPa and 2.74 GPa at 650 °C, and between 2.70 GPa and 2.72 GPa at 680 °C. The brackets at lower temperatures were broader because of the slower reaction rate. In Fig. 1 the position of the equilibrium is approximated by a straight dashed line between the experimental brackets. The two solid lines show the limiting positions between which the reaction could occur, taking into account the uncertainties in pressure and temperature indicated. The reaction should not be exactly linear in *P-T* space since the thermodynamic properties of water, and possibly also the water content of the sanidine hydrate, vary along the phase boundary.

Small quantities of coesite formed in all the reversal experiments that were at a high enough pressure to crystallise sanidine hydrate (Table 2). The formation of coesite may affect the reversal results. It is also possible that quartz was a by-product in some of the lower pressure experiments. However, quartz would not be apparent in small quantities in a powder XRD pattern in the presence of sanidine, as the quartz peaks would be masked by larger sanidine peaks. The quartz-coesite boundary is almost coincident with the sanidine–sanidine hydrate reaction and therefore only coesite was found in the presence of sanidine hydrate. Two experimental run products were doped with coesite prior to X-ray diffraction in order to quantify the amount of coesite present. The increase in intensity of the coesite peaks showed that both had contained less than 3 wt% of coesite prior to doping. The XRD traces of these experiments showed similarly sized coesite peaks to the

Table 2 Reversal experiments on the reaction between sanidine and water to form sanidine hydrate

Run	*P* (Gpa)	*T* (° C)	H_2O (wt %)	Length (hours)	Type[a]	Starting material[b]	Results[c]
50	2.855	550	5.88	24.5	pcR	PTmix	Only SH with coes
51	2.000	550	6.36	24.0	pcR	PTmix	San only no SH or coes
52	2.667	550	6.09	25.0	pcR	PTmix	≈75% SH but still some san + coes
53	2.300	550	6.43	24.0	pcR	PTmix	San only no SH or coes
54	2.400	550	6.26	24.5	pcR	PTmix	≈20% SH = mostly san – no coes
55	2.590	550	7.05	24.5	pcR	PTmix	≈60% SH but still some san + coes
56	2.855	650	6.28	24.0	pcR	PTmix	SH + coes only
57	2.500	650	6.35	24.5	pcR	PTmix	San only – no coesite
58	2.667	650	6.15	42.0	pcR	PTmix	San only – possible slight trace of coes
59	2.737	650	6.22	24.0	pcR	PTmix	≈90% SH but still some san + coes
60	2.350	450	6.36	168	pcR	PTmix	≈10% SH – mostly san – no coes
61	2.721	680	6.67	20.0	pcR	PTmix	All SH – coesite present
62	2.696	680	6.38	24.0	pcR	PTmix	Mostly san but traces of SH + coes
65	2.500	550	6.9	63.0	pcR	PTmix	≈20% SH – mostly san – no coes
68	2.500	450	9.1	168	pcR	PTmix	≈55% SH but still some san + coes

[a] (*pc* piston cylinder apparatus, *R* reversal experiment)
[b] (*PTmix* mixture of 40% sanidine hydrate and 60% sanidine)
[c] (*SH* sanidine hydrate, *san* sanidine, *coes* coesite)

other experiments, suggesting that the quantity of coesite was small in all experiments.

The formation of coesite in the synthesis experiments is not easily explained. The gel may have contained an excess of silica, the water in the capsule may have dissolved the gel incongruently encouraging the precipitation of quench coesite, or the sanidine hydrate may have been silica deficient relative to stoichiometric $KAlSi_3O_8 \cdot nH_2O$ perhaps due to hydrogrossular like substitution. However, since the quantity of coesite was small, the problem is considered unlikely to affect the overall results.

The reversal experiments are compared with the unreversed synthesis experiments of Seki and Kennedy (1964a) in Fig. 1. Their synthesis boundary was at lower pressure and has a steeper gradient than the one determined here. Their experiments involved synthesis from a gel or glass starting material, in runs of ≤3 hours duration. It is possible that these short experiments produced metastable products as was seen in the $BaAl_2Si_2O_8$–H_2O system (Graham et al. 1992). To test this hypothesis two experiments were performed to reproduce Seki and Kennedy's conditions. Run 67 (Fig. 1) was a synthesis experiment of only three hours duration at 2.350 GPa and 550 °C, between the positions for the reaction given by Seki and Kennedy and that found in the present study; this produced sanidine but no metastable sanidine hydrate. The experiment was then repeated (run 71) using a gel starting material seeded with crystals of sanidine hydrate. After two hours the sanidine hydrate seeds had disappeared and only sanidine was present. Thus Seki and Kennedy's results were not reproduced. The discrepancy between these results and those of Seki and Kennedy may be caused by variations in the apparatus, problems with pressure or temperature calibration, or the effect of different starting materials. Seki and Kennedy used either pure sanidine crystallised from a $KAlSi_3O_8$ glass or a natural sanidine (4.40% Na_2O, 11.7% K_2O), whereas $KAlSi_3O_8$ gel was used for synthesis experiments in the present study.

Water content of sanidine hydrate

Infrared spectroscopy

Infrared spectroscopy provided evidence of the nature and speciation of water in the hydrate structure. Two typical infrared spectra of sanidine hydrate are shown in Fig. 2. At 1610 cm^{-1} an absorption peak (or transmission trough) indicates the presence of molecular H_2O. In the OH stretching region two sharp absorption peaks at 3530 and 3620 cm^{-1} confirm the presence of isolated structurally bound H_2O molecules. In the OH stretching region of the spectra there is also a broad background hump at a slightly lower frequency which indicates the existence of surface water or water held within micropores. Samples were also investigated in the near infrared at wavenumbers between 4000 and 5800 cm^{-1} in order to look for overtones of these fundamental vibrations seen at lower wavenumbers. However, no combination modes were seen above noise level, and therefore no additional information on the nature of the structural water could be obtained.

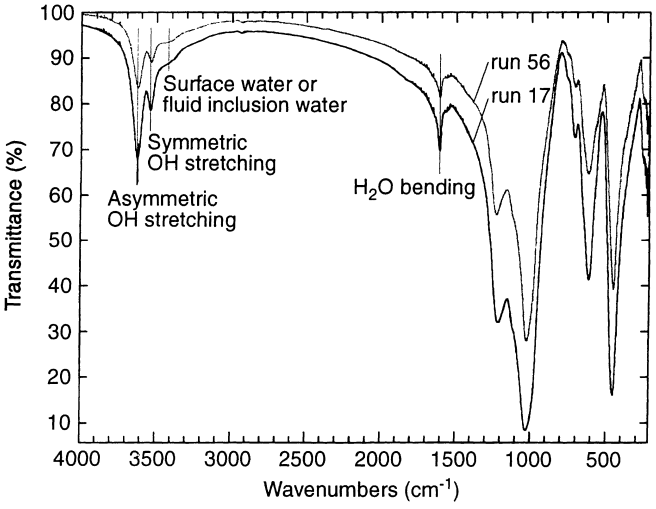

Fig. 2 Infrared spectra of two samples of sanidine hydrate. The fainter top trace is of run 56 and the lower darker one is that of run 17 (see Table 3)

The spectrum for sanidine hydrate contains only two peaks in the OH stretching region. This probably indicates that, unlike cordierite (Goldman et al. 1977) or beryl (Schmetzer and Kiefert 1990) which have different types of H_2O channel sites, there is only one H_2O site in sanidine hydrate.

Infrared spectra for sanidine hydrate are similar to spectra for cymrite prepared at 0.965 GPa and 740 °C (Graham et al. 1992). The positions of the OH stretching absorption peaks in sanidine hydrate are shifted to higher frequencies (larger wavenumbers) than in cymrite but not to such high frequencies as are found in cordierite or beryl. This frequency shift implies that the strengths of the bonds holding the H_2O molecules in the sanidine hydrate structure are slightly stronger than those in cymrite, but not as strong as those in cordierite or beryl.

Spectroscopic evidence for structurally bound OH groups is difficult to observe when frequencies lie in the range of OH stretching of an H_2O molecule. However, samples of sanidine hydrate dehydrated at 800 °C showed no residual OH stretching attributable to OH groups. Thus if OH groups were present in sanidine hydrate they must be removed on dehydration at temperatures less than 800 °C.

Thermogravimetric analysis

Typical results of a thermogravimetric analysis of a sanidine hydrate sample (run 17) are shown in Fig. 3. All the thermogravimetric analyses exhibited a similar shaped curve. Up to ~300 °C there was a very slight and variable weight loss. Between 300 and 550 °C there was

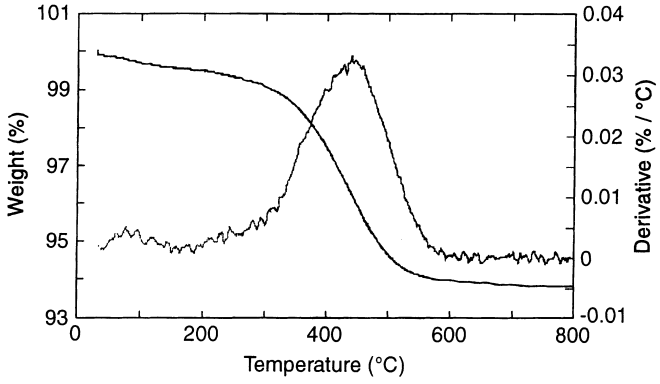

Fig. 3 A typical thermogravimetric result of a sanidine hydrate sample (run 17) showing the weight loss (*heavier black line*) and the derivative of the weight loss with respect to temperature (*fainter grey line*) plotted against temperature

a substantial loss of weight. From 550 to ~800 °C the weight sometimes appeared to drop slightly, by less than 0.3 wt%, but up to 1000 °C the weight then appeared to rise again slightly. The first derivative of the weight loss with respect to temperature was plotted to further clarify the changes in slope. These samples showed only one strong peak in the derivative in the 300–550 °C region and a minimal one below 300 °C. The apparent small weight increase above 800 °C is probably due only to measurement drift as seen when samples of anhydrous phases are run. Samples were checked by infrared spectroscopy and showed no remaining structural OH peaks after dehydration to 800 °C.

To calculate the percentage weight loss over a particular weight loss event, two positions were chosen on the curve outside the temperature range of the weight loss, where $d(wt\%)/dT$ was at a minimum. Tangents were drawn at these two positions and another at the point of inflection where $d(wt\%)/dT$ was at a maximum. The two points of intersection of these three tangents were then used to measure the weight loss without the effect of the background of measurement drift and weight loss from other events.

The weight loss exhibited by sanidine hydrate can be interpreted as three weight loss events over the temperature ranges 0–300 °C, 300–550 °C and 550–800 °C (Table 3). Loss at ≤300 °C is thought to be due to surface water. The major weight loss event between 300 and 500 °C is taken to represent the loss of structural H_2O as identified using infrared spectroscopy (see previous section). Above 550 °C but below 800 °C the small observed weight loss in some of the samples may be that of a small amount of structural OH, as was suggested by Graham et al. (1992) for a similar weight loss observed in cymrite.

Unlike the behaviour of cymrite (Graham et al. 1992), sanidine hydrate shows no obvious systematic variation in percentage weight loss with pressure and temperature of synthesis within the range studied. Values range irregularly from 4.42 to 5.85 wt%. Repeat thermogravimetric runs on the same samples showed that differences in the percentage weight loss within the same sample were almost within the measurement error of the equipment (± 0.1 wt%). However, samples synthesised at similar pressures and temperatures showed larger differences. The overall difference between runs was greater than ± 0.1 wt%, and perhaps of the order of ± 0.3 wt%. This discrepancy is thought to be caused by platinum contamination of the samples rather than measuring errors in the thermogravimetric equipment. However, it is interesting to note that the weight loss between 300 and 550 °C in all samples was within ± 0.8 wt% of the mean value of 5.07 wt%. In addition, the maximum value of weight loss in this event is less than the weight percentage of H_2O equivalent to one H_2O molecule per formula unit (6.07 wt%).

Attempts to quantify the platinum contamination within the samples using atomic absorption analysis did not fully explain the variation seen in the thermogravimetric data. However, platinum contamination in all samples tested had the effect of decreasing the apparent weight percentages of the main water loss event by 0.2 to 0.3 wt%. Any agreement between the three repeated runs was not improved by a corrected weight figure and therefore it is probable that some of the platinum was lost prior to atomic absorption analysis. Thus the thermogravimetric data constrain only minimum values of water content.

Table 3 Table of apparent percentage weight losses of samples of sanidine hydrate measured by thermogravimetric analysis. These values represent the minimum percentages of water lost in each temperature interval as samples were generally contaminated with variable amounts of platinum

Run number	*P* of synthesis (Gpa)	*T* of synthesis (° C)	Weight loss (0–300° C) (%)	Weight loss (300–550° C) (%)	Weight loss (550–800° C) (%)
72.1	2.855	450	0.51	5.38	0.31
50.1	2.855	550	0.03	4.77	0.28
50.2	2.855	550	0.25	4.81	0.31
22.1	2.868	550	0.56	5.07	0.5
17.1	2.923	550	0.61	5.27	0.03
16.1	2.930	550	0.51	5.85	0.00
56.1	2.855	650	0.75	4.50	0.37
56.2	2.855	650	0.90	4.42	0.29
77.1	2.855	680	0.60	4.66	0.27
77.2	2.855	680	0.35	4.42	0.27
75.1	2.737	500	0.34	5.42	0.13
76.1	2.737	600	0.27	5.15	0.27
61.1	2.721	680	0.89	4.59	0.37

The anhydrous product of dehydration of sanidine hydrate above 800 °C produced by heating during thermogravimetric analysis has hexagonal symmetry and similar cell dimensions to sanidine hydrate (see below). It is in all respects analogous to the hexacelsian ($BaAl_2Si_2O_8$) formed from dehydration of cymrite in the system $BaAl_2Si_2O_8$–H_2O (Graham et al. 1992; Viswanathan et al. 1992). This phase has not been identified or described before, and is here called hexasanidine, emphasising its similarity to hexacelsian. Hexasanidine forms during thermogravimetric analysis at high temperature and low pressure where sanidine is known to be the stable phase (Schairer and Bowen 1955) and may form metastably in an analogous manner to hexacelsian. Hexacelsian ($BaAl_2Si_2O_8$) exists stably only above 1590 °C at atmospheric pressure (Lin and Foster 1968), and hence does not occur naturally. Below this temperature hexacelsian (hexagonal $BaAl_2Si_2O_8$) exists metastably down to 300 °C (Lin and Foster 1968). The hexagonal double-layer aluminosilicate structure of cymrite and hexacelsian has a ready tendency to crystallise and persist metastably (Graham et al. 1992; Viswanathan et al. 1992).

Unit cell parameters

Figure 4 shows a comparison of the typical XRD trace for sanidine hydrate and hexasanidine in the 0 to 60°2θ angle range. Small shifts in the peak positions indicate small differences in the unit cell dimensions (Tables 4 and 5). The small variations observed in unit cell parameters between samples were not systematically related to the conditions of synthesis in the *P*-*T* range investigated here. Repeat calculations for four of the samples using different aliquots of the same sample showed that variation between different samples and repeat runs of the same sample were of a similar order of magnitude. All calculated unit cell parameters lay within a range of ±0.0006 nm of the mean values.

The mean values for the cell parameters for sanidine hydrate and hexasanidine are given in Table 6. The changes in cell parameters from samples with an average water content of 0.83 moles per formula unit (sanidine hydrate) to samples with no water in their structure after

Table 4 Unit cell parameters calculated using a hexagonal primitive cell, for samples of sanidine hydrate synthesised at various pressures and temperatures. Numbers given in brackets are ±1σ variations obtained from the programme CELLREF

Run	*P* (Gpa)	*T* (° C)	*a* (nm)	*c* (nm)	Volume (nm^3)
16a	2.930	550	0.53370(4)	0.77050(5)	0.19006(2)
16b	2.930	550	0.53372(4)	0.77115(15)	0.19023(4)
17	2.923	550	0.53366(4)	0.77142(15)	0.19026(5)
22	2.879	550	0.53368(5)	0.77109(16)	0.19019(5)
50a	2.855	550	0.53382(5)	0.77179(19)	0.19046(6)
72	2.855	450	0.53381(4)	0.77089(15)	0.19024(4)
56a	2.855	650	0.53363(4)	0.77180(15)	0.19033(4)
56b	2.855	650	0.53380(8)	0.77101(30)	0.19033(9)
77	2.855	680	0.5335(3)	0.7716(10)	0.1901(3)
75	2.737	500	0.53381(8)	0.77122(30)	0.19032(9)
76	2.737	600	0.53344(5)	0.77121(18)	0.19005(5)
61a	2.721	680	0.53356(4)	0.77176(12)	0.19027(4)
61b	2.721	680	0.53355(5)	0.77192(12)	0.19030(4)
Mean			0.53366	0.77141	0.19026
Range			±0.00022	±0.00052	±0.00020

Table 5 Unit cell parameters calculated using a hexagonal primitive cell, for samples of hexasanidine synthesised by dehydrating samples of sanidine hydrate using thermogravimetric analysis. Numbers given in brackets are ±1σ variations obtained from the programme CELLREF

Run	*P* (Gpa)	*T* (° C)	*a* (nm)	*c* (nm)	Volume (nm^3)
61	2.721	680	0.52895(7)	0.78149(38)	0.18935(7)
72	2.855	450	0.52894(7)	0.78192(6)	0.18945(5)
75	2.737	500	0.52878(6)	0.78215(5)	0.18939(4)
76	2.737	600	0.52880(6)	0.78216(5)	0.18941(4)
16a	2.830	550	0.52908(7)	0.78182(40)	0.18952(9)
16b	2.930	550	0.52891(7)	0.78180(5)	0.18940(5)
17a	2.923	550	0.52889(4)	0.78178(3)	0.18938(3)
17b	2.923	550	0.52909(10)	0.78170(8)	0.18950(7)
Mean			0.52893	0.78185	0.1895
Range			±0.00016	±0.00036	±0.0001

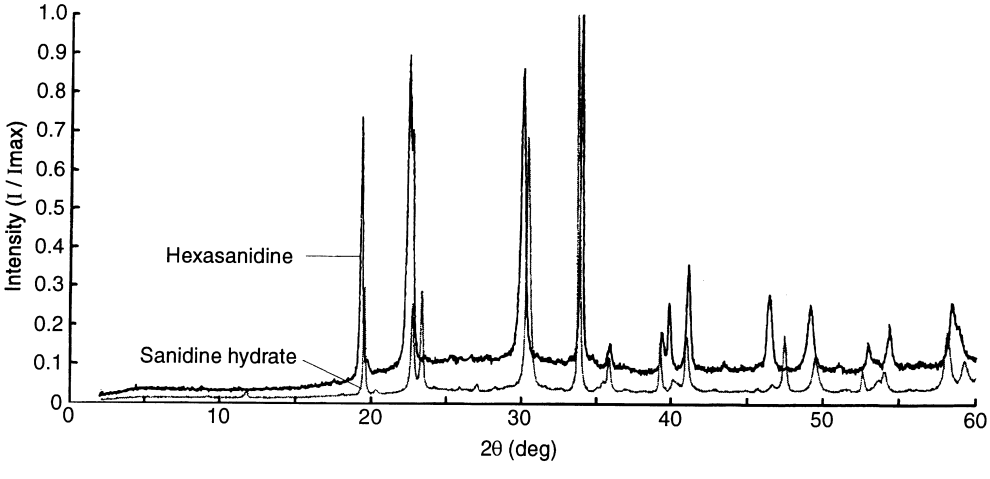

Fig. 4 A comparison of the powder XRD patterns for sanidine hydrate (run 56, shown in *grey*) and "hexasanidine" (run 61, shown in *black*). A smaller quantity of sample was used for the hexasanidine and so a larger proportion of the background is from the glass mounting slide

dehydration (hexasanidine) are $\Delta a = -0.00473$ ($\pm$ 0.00016) nm and $\Delta c = 0.01044$ (± 0.00063) nm. Hence any slight variation in the cell parameters as a result of variation in the water content would be hard to detect from the cell dimensions. Comparison of these cell parameters with those calculated by Viswanathan et al. (1992) for cymrite and hexacelsian shows similar values and a similar contraction in the *a* direction and expansion in the *c* direction of the unit cell (Table 6) upon dehydration. The fact that hexasanidine can be synthesised shows that the water content of sanidine hydrate may in fact vary even though this was not seen in the *P-T* range studied.

Discussion: the geological significance of sanidine hydrate

Pressure-temperature constraints

The results of this study constrain the lower pressure stability limit for sanidine hydrate in the presence of water. Thermodynamic analysis showed the data given above were not sufficiently well constrained to extrapolate the reaction reliably outside the bracketed region (Thompson 1995) although values of the average enthalpy and entropy of reaction over the *P-T* range studied ($\Delta H°_{(r)<T>} = 18000$ (± 5000) J mol^{-1} and $\Delta S°_{(r)<T>} = 92.75$ (± 5.80) J K^{-1}mol^{-1} for an average water content of $n = 0.83$ in the sanidine hydrate formula) were found to be very similar to those for the cymrite to celsian reaction (Graham et al. 1992). At temperatures higher than those investigated, sanidine hydrate should melt in the presence of excess water. The temperature of this melting has not been determined. However, the position of the wet melting curve of sanidine is known from the work of Goldsmith and Peterson (1990) (Fig. 5). The results of their melting experiments at high pressures, in excess of 1.5 Gpa, were ambiguous due to the presence of what the authors called a "granular incoherent brownish isotropic substance" (GIBIS) which was indistinguishable from the melt phase and thought to have quenched from the vapour phase. The formation of GIBIS could indicate the supercritical behaviour of the fluid at these pressures and temperatures when the vapour phase and the melt become indistinguishable. Goldsmith and Peterson postulated that the presence of GIBIS could be due to the incongruent solubility of the sanidine or microcline starting material in the vapour phase at high pressure. In this case the melting sanidine

Table 6 A comparison of the cell parameters for sanidine hydrate, hexasanidine, cymrite, and hexacelsian. Data for cymrite and hexacelsian are taken from Viswanathan et al. (1992). Errors shown for sanidine hydrate and hexasanidine are the ranges shown in Tables 4 and 5

	a (nm)	Δa	*c* (nm)	Δc
Sanidine hydrate	0.53366(22)		0.77141(52)	
Hexasanidine	0.52893(16)	−0.00473(27)	0.78185(36)	0.01044(63)
Cymrite	0.5343(1)		0.7681(2)	
Hexacelsian	0.5298(2)	−0.0045(2)	0.7790(5)	0.00109(5)

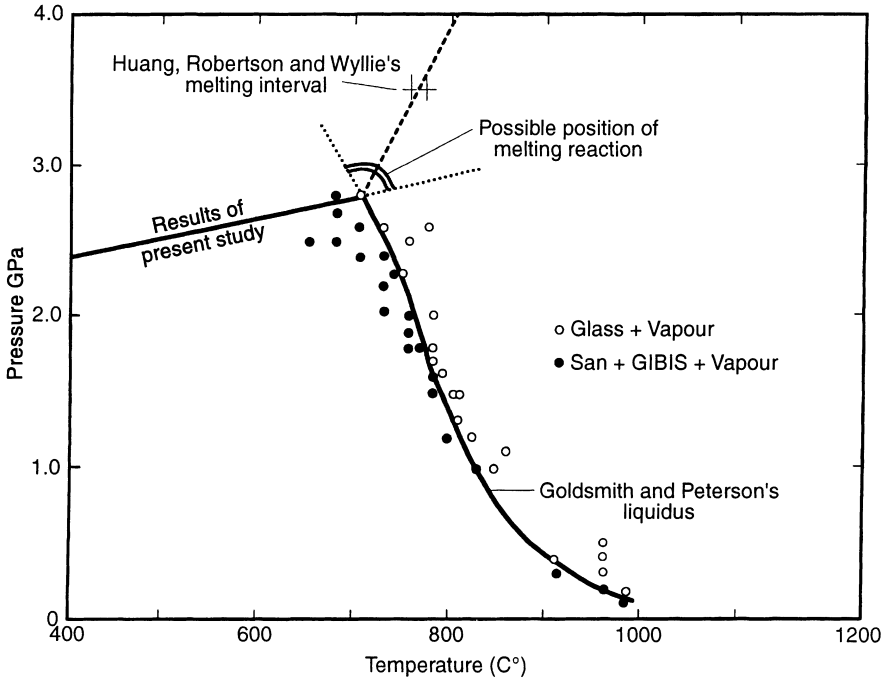

Fig. 5 A comparison of the results from the present study with the position of the liquidus as determined by Goldsmith and Peterson in 1990. The melting curve of sanidine hydrate must lie between the metastable extensions of these two curves, perhaps in the position shown by the *dotted line*. The melting interval of Huang, et al. (1973) may indicate that the reaction occurs between these temperatures although this is not a reversed reaction

would no longer be univariant, explaining the occurrence of GIBIS and hence a melting interval over a fairly broad temperature range of over 130 °C at 2.5 GPa. Despite these problems they determined a line (shown in Fig. 5) corresponding to the temperature at which crystals could no longer be seen within the GIBIS which was their best approximation for the sanidine liquids. Above 1.5 Gpa none of their experiments gave wholly crystalline products and the solidus position could not be determined.

In the synthesis and reversal experiments described here, carried out at similar pressures and temperatures to the experiments performed by Goldsmith and Peterson, there was little positive evidence for a substance comparable to GIBIS near the liquidus. All samples from both synthesis and reversal experiments, including those from the lowest temperature reversal experiments at 450 °C, contained small amounts of brownish material. This material may have been amorphous, perhaps formed during quenching from the vapour, although it was impossible to confirm this. Even samples from the lowest temperature reversal experiments at 450 °C contained this material and so it seems unlikely that this material is a product of melting. Investigation of some of the samples formed well below the liquidus using scanning electron microscopy showed material which looked like Goldsmith and Peterson's GIBIS. In the present study only very small excesses of water were present, while the experiments of Goldsmith and Peterson (1990) contained unspecified but much larger amounts of water necessary to saturate the high pressure melts. Therefore the much smaller amounts of material quenched from the melt are to be expected in the present experiments compared to those of Goldsmith and Peterson, and the apparent absence or scarcity of GIBIS in our study is not surprising. The melting of sanidine hydrate is therefore restricted to the approximate position of the dotted line shown in Fig. 5 between the metastable extensions of the two curves. Huang et al. (1973) found melting to occur, in an unreversed experiment, between 760 and 780 °C at 3.5 GPa, which would restrict the stability field of sanidine hydrate to temperatures of less than ~400–1000 °C in the pressure range of 2.3–4.0 GPa, i.e. at depths of 70–120 km.

To achieve these conditions in nature would require a low geothermal gradient of < 6.5 °C km^{-1} (corresponding to a surface heat flow of < 40 mW m^{-2}). Occasional evidence for such low geothermal gradients has been found in measured heat flows at the surface (Pollack and Chapman 1977) and in geothermal gradients calculated from xenoliths in kimberlite pipes (Boyd 1984; Smyth and Hatton 1977), but they would be most common in subduction zones. Hydrous fluids required to stabilise sanidine hydrate would also be available. The *P-T* conditions deduced for ancient subduction zones are almost suitable to form sanidine hydrate. These are rare, perhaps because of the difficulty of bringing such rocks to the surface without major mineralogical modification. Ultra-high pressure rocks of the Dora Maira massif in the Western Alps formed at very low geothermal gradients of possibly 7–8 °C km^{-1} at 2.8–3.5 GPa and 700–800 °C (Schreyer et al. 1987), close to the limit of sanidine hydrate stability. Therefore it should be possible to subduct rocks into the sanidine hydrate stability field. However, the bulk compositions of the Dora Maira rocks are not appropriate to stabilise sanidine hydrate even if other conditions were favourable.

Numerical simulations of subduction zone *P-T*-time paths may help to constrain the occurrence of the *P-T* conditions required for the stability of sanidine hydrate. The two-dimensional finite difference model of Peacock (1991) simulates the heat transfer in a subduction zone with a dip of 26.6° and indicates that the *P-T* conditions required for the formation of sanidine hydrate are more likely to be attained in a subduction zone if: (1) the subducting oceanic crust is at least 100 Ma old; (2) the slab has subducted at least 600 km of material since its formation; (3) the rock is either in the base of the oceanic crust or in parts of the mantle wedge that are not dragged down by the subducting slab; or (4) the rock is in the top of the slab after a lot of crust has subducted when there is no convection in the mantle wedge.

Compositional constraints

The system K_2O-Al_2O_3-SiO_2-H_2O, in which the present experiments have been performed, is a simple one with only four components and three phases in the *P-T* range studied. Natural multi-component rocks are inevitably more complex. Whether sanidine hydrate may form by reactions between phases other than either sanidine and vapour, or from crystallising a water rich sanidine melt, is not known. However, in most bulk rock compositions the stability of sanidine is restricted by many reactions which occur at lower pressures (Thompson 1995). Under pressure and temperature conditions of over 2.0–3.0 GPa and below 700–1000 °C (the approximate stability field for sanidine hydrate), sanidine would not be stable in the presence of:

Forsterite	Wendlandt and Eggler (1980)
Talc + vapour	Massonne (1992), Wendlandt and Eggler (1980)
Phlogopite + vapour	Massonne (1992)
Cordierite + vapour	Massonne and Schreyer (1987)
Enstatite + vapour	Wood (1976), Luth (1967)
Enstatite + liquid	Bohlen et al. (1983)
Forsterite + vapour	Luth (1967)
Tremolite + Co_2 rich vapour	Hewitt (1975)
Corundum + vapour	Huang et al. (1973)
Sillimanite/kyanite + vapour	Luth (1967)

Although the absence of sanidine does not prohibit the occurrence of sanidine hydrate, the reactions listed above may limit the range of rock compositions capable of hosting sanidine hydrate. Most bulk compositions of rock would have an excess of these phases relative to

sanidine and hence sanidine would be exhausted on metamorphism prior to the conditions required to form sanidine hydrate. If a large excess of free water is available, sanidine will react with the vapour to form muscovite (Seki and Kennedy 1965), or at higher pressures but lower water contents, sanidine hydrate may dissolve in the vapour phase (Stern and Wyllie 1981). In addition any melt present would take up available free water (Huang and Wyllie 1975) lowering water activities and further restricting the stability of sanidine hydrate.

Some evolved igneous rocks contain a large proportion of potassium feldspar with only relatively small proportions of these other phases. The only rock types that have been studied extensively at high pressures and temperatures are synthetic granite compositions, in which many of the relevant reactions have not been reversed (Huang et al. 1973; Huang and Wyllie 1974, 1975). Not much is known about the phase relations of other high pressure evolved igneous rock types rich in potassium feldspar, such as syenites. The subduction of rocks with a granitic composition is probably uncommon and not likely to occur in the coldest parts of a subduction zone at the base of the oceanic crust or mantle wedge. The water content of the rock must be sufficiently high to form sanidine hydrate, or sanidine will persist until it reacts to form the wadeite type phase described by Kinomura et al. (1975).

Concluding remarks

1. The position of the reaction between sanidine and water to form sanidine hydrate lies between the four brackets of 2.35 and 2.5 Gpa at 450 °C, 2.4 and 2.59 Gpa at 550 °C, 2.67 and 2.74 Gpa at 650 °C, and 2.70 and 2.72 GPa at 680 °C.
2. The predominant water species in sanidine hydrate is molecular H_2O held within one site in the crystal structure.
3. The apparent quantity of this structural H_2O varied between 4.42 and 5.85 wt%. These apparent values for structural H_2O represent minimum values as the samples were contaminated with platinum when they were extracted from the capsule in the piston cylinder experiments. The average value corresponded with $n = 0.83$ in the formula $KAlSi_3O_8 \cdot nH_2O$.
4. No systematic variation in structural water content in sanidine hydrate with the pressure and temperature of synthesis was detected, perhaps because the platinum contamination obscured any systematic behaviour. However, it was shown that the water could be removed entirely from sanidine hydrate by dehydration to create a metastable, anhydrous, hexagonal $KAlSi_3O_8$ phase, hexasanidine. The measured water content of sanidine hydrate did not exceed one molecule of H_2O per formula unit. Therefore it is probable that a solid solution exists between $KAlSi_3O_8 \cdot H_2O$ and hexagonal $KAlSi_3O_8$ in a similar manner to that found between cymrite and hexacelsian in the system $BaAl_2Si_2O_8$–H_2O.
5. The unit cell parameters for sanidine hydrate were $a = 0.53366$ (± 0.00022) nm and $c = 0.77141$ (± 0.00052) nm and for hexasanidine were $a = 0.52893$ (± 0.00016) nm and $c = 0.78185$ (± 0.00036) nm.

Acknowledgements We thank Bob Brown for laboratory support and Nic Odling and Steve Elphick for experimental advice and encouragement throughout this project. Infrared spectroscopy was conducted in the National Museum of Scotland, Edinburgh. Thermogravimetric analyses were performed in the Department of Chemistry at the University of St Andrews. Dr P.E. Champness of Manchester University provided the program CELLREF used for calculating the cell parameters. The gel starting material was made by Dr D.L. Hamilton also at Manchester. Dr Michael Carpenter and an anonymous reviewer are thanked for constructive comments. The Experimental Petrology Laboratories are supported by the Natural Environment Research Council. The work was carried out during tenure of a NERC Research Studentship by Pauline Thompson.

References

Bohlen SR, Boettcher AL (1982) The quartz–coesite transformation: a precise determination and the effects of other components. J Geophys Res 87: 7073–7078

Bohlen SR, Boettcher AL, Wall VJ, Clemens JD (1983) Stability of phlogopite-quartz and sanidine-quartz: a model for melting in the lower crust. Contrib Mineral Petrol 83: 270–277

Bose K, Ganguly J (1995) Quartz–coesite transition revisited: reversed experimental determination at 500–1200 °C and retrieved thermochemical properties. Am Mineral 80: 231–238

Boyd FR (1984) Siberian geotherm based on Iherzolite xenoliths from the Udachnaya kimberlite, USSR. Geology 12: 528–530

Brown WL, Parsons I (1989) Alkali feldspars: ordering rates, phase transformations and behaviour diagrams for igneous rocks. Mineral Mag 53: 25–42

Carpenter MA, Salje EKH (1994) Thermodynamics of non-convergent cation ordering in minerals. III. Order parameter coupling in potassium feldspar. Am Mineral 79: 1084–1098

Drits VA, Kashaev AA, Sokolova GV (1975) Crystal structure of cymrite. Kristallografiya 20: 280–286

Goldman DS, Rossman GR, Dollase WA (1977) Channel constituents in cordierite. Am Mineral 62: 1144–1157

Goldsmith JR, Peterson JW (1990) Hydrothermal melting behaviour of $KAlSi_3O_8$ as microcline and sanidine. Am Mineral 75: 1362–1369

Graham GM, Tareen JAK, Macmillan PF, Lowe BM (1992) An experimental and thermodynamic study of cymrite and celsian stability in the system BaO-Al_2O_3-SiO_2-H_2O. Eur J Mineral 4: 251–269

Hamilton DL, Henderson CMB (1968) The preparation of silicate compositions by a gelling method. Mineral Mag 36: 832–838

Hewitt DA (1975) Stability of the assemblage phlogopite-calcite-quartz. Am Mineral 60: 391–397

Hsu LC (1994) Cymrite: new occurrence and stability. Contrib Mineral Petrol 118: 314–320

Huang WL, Wyllie PJ (1974) Melting relations of muscovite with quartz and sanidine in the K_2O-Al_2O_3-SiO_2–H_2O system to 30 kbar and an outline of paragonite melting relations. Am J Sci 274: 378–395

Huang WL, Wyllie PJ (1975) Melting reactions in the system $NaAlSi_3O_8$-$KAlSi_3O_8$-SiO_2 to 35 kbar, dry and with excess water. J Geol 83: 737–748

Huang WL, Robertson JK, Wyllie PJ (1973) Melting relations of muscovite to 30 kbar in the system $KAlSi_3O_8$–Al_2O_3-H_2O. Am J Sci 273: 415–427

Kinomura N, Kume S, Koizumi M (1975) Synthesis of $K_2SiSi_3O_9$ with silicon in 4- and 6- co-ordination. Mineral Mag 40: 401–404

Lin HC, Foster WR (1968) Studies in the system BaO-Al_2O_3-SiO_2-H_2O. Am Mineral 53: 134–144

Luth WC (1967) Studies in the system $KAlSiO_4$-Mg_2SiO_4-SiO_2-H_2O. I. Inferred phase relations and petrologic applications. J Petrol 8: 372–416

Massonne HJ (1992) Evidence for low temperature ultrapotassic siliceous fluids in the subduction zone environments from experiments in the system K_2O-MgO-Al_2O_3-SiO_2-H_2O (KMASH). Lithos 28: 421–434

Massonne HJ, Schreyer W (1987) Phengite geobarometry based on the limiting assemblage with K-feldspar, phlogopite and quartz. Contrib Mineral Petrol 96: 212–224

Moles N (1985) Metamorphic conditions and uplift history in central Perthshire: evidence from mineral equilibria in the Foss celsian-barite-sulphide deposit, Aberfeldy. J Geol Soc London 142: 39–52

Nitsch KH (1980) Reaktion von Barium Feldspat (Celsian) mit H_2O zu Cymrite unter metamorphen Besdingungen. Fortschr Mineral 58 Beih: 98–100

Peacock SM (1991) Numerical simulation of subduction zone pressure-temperature-time paths: constraints on fluid production and arc magmatism. Philos Trans R Soc London 335: 341–353

Pollack HN, Chapman DS (1977) On the regional variation of heat flow, geotherms, and lithospheric thickness. Tectonophysics 38: 279–296

Schairer JF, Bowen NL (1955) The system K_2O-Al_2O_3-SiO_2. Am J Sci 253: 681–746

Schmetzer K, Kiefert L (1990) Water in beryl – a contribution to the separability of natural and synthetic emeralds by infrared spectroscopy. J Gemmol 22: 215–223

Schreyer W, Massonne HJ, Chopin C (1987) Continental crust subducted to depths near 100 km: implications for magma and fluid genesis in collision zones: magmatic processes: physiochemical principles. Geochem Soc Spec Publ No 1

Seki Y, Kennedy GC (1964a) The breakdown of potassium feldspar $KAlSi_3O_8$ at high temperatures and high pressures. Am Mineral 19: 1688–1708

Seki Y, Kennedy GC (1965) Phase relations between cymrite, $BaAlSi_3O_8(OH)$, and celsian, $BaAlSi_3O_8$ Am Mineral 49: 1407–1426

Seki Y, Kennedy GC (1965) Muscovite and its melting relations in the system $KAlSi_3O_8$-H_2O. Geochim Cosmochim Acta 29: 1077–1083

Smyth JR, Hatton CJ (1977) A coesite-sanidine grosopydite from the Roberts Victor kimberlite. Earth Planet Sci Lett 34: 284–290

Stern CR, Wyllie PJ (1981) Phase relationships of I-type granite. J Geophys Res 86: 10412–422

Thompson P (1994) The sanidine "sanidine hydrate" reaction. Mineral Mag 58: 897

Thompson P (1995) The behaviour of potassium feldspar at high water pressures (unpublished). PhD thesis, Univ Edinburgh

Viswanathan K, Harniet O, Epple M (1992) Hydrated barium aluminosilicates, $BaAl_2Si_2O_8 \cdot nH_2O$, and their relations to cymrite and hexacelsian. Eur J Mineral 4: 271–278

Wendlandt RF, Eggler DH (1980) The origin of potassic magmas. 2. Stability of phlogopite in natural spinel lherzolite and in the system $KAlSiO_4$-MgO-SiO_2-H_2O-CO_2 at high pressures and temperatures. Am J Sci 280: 421–458

Wood BJ (1976) The reaction phlogopite + quartz = enstatite + sanidine + H_2O. In: Biggan GM (ed) Progress in experimental petrology. Nat Environ Res Counc G B Ser D, pp 17–19

Wright TL (1968) X-ray and optical study of alkali feldspar. II. An X-ray method for determining the composition and structural state from measurement of 2θ values for three reflections. Am Mineral 53: 88–104